

# SUSY Long-Lived Massive Particles: Detection and Physics at the LHC

S. Ambrosanio <sup>a,1</sup>, B. Mele <sup>b,c</sup>, A. Nisati <sup>b,c</sup>, S. Petrarca <sup>c,b</sup>,  
G. Polesello <sup>d</sup>, A. Rimoldi <sup>d,e</sup>, G. Salvini <sup>c,b</sup>

<sup>a</sup> CERN – *Theory Division, CH-1211 Geneva 23, Switzerland*

<sup>b</sup> INFN – *Sezione di Roma I, c/o Dipartimento di Fisica, Università “La Sapienza”,  
p. le Aldo Moro 2, I-00185 Roma, Italy*

<sup>c</sup> *Dipartimento di Fisica, Università “La Sapienza”,  
p. le Aldo Moro 2, I-00185 Roma, Italy*

<sup>d</sup> INFN – *Sezione di Pavia e Dip. Fis. Nucl. Teor., Università di Pavia,  
via Bassi 6, I-27100 Pavia, Italy*

<sup>e</sup> CERN – *EP Division, CH-1211 Geneva 23, Switzerland*

## Abstract

We draw a possible scenario for the observation of massive long-lived charged particles at the LHC detector ATLAS. The required flexibility of the detector triggers and of the identification and reconstruction systems are discussed. As an example, we focus on the measurement of the mass and lifetime of long-lived charged sleptons predicted in the framework of supersymmetric models with gauge-mediated supersymmetry (SUSY) breaking. In this case, the next-to-lightest SUSY particle can be the light scalar partner of the tau lepton ( $\tilde{\tau}_1$ ), possibly decaying slowly into a gravitino. A wide region of the SUSY parameters space was explored. The accessible range and precision on the measurement of the SUSY breaking scale parameter  $\sqrt{F}$  achievable with a counting method are assessed.

Submitted for publication to *Rendiconti dei Lincei*

---

<sup>1</sup> Address after 1–Jan–2001:

Banca di Roma, Direzione Generale, Linea Finanza, viale U. Tupini 180, I-00144 Roma, Italy



# 1 Introduction

The Large Hadron Collider (LHC) at the European Laboratory for Particle Physics (CERN) in Geneva has an enormous and unique potential of discovering new particles beyond the Standard Model (SM) over a large mass range around the TeV scale.

In this article, we consider an interesting class of exotic particles that are characterised by a few model independent common features:

- a) they have large masses and are produced with  $\beta < 1$  in a non negligible fraction of events at the LHC;
- b) they are stable or quasi-stable, i.e. their lifetime is larger than  $10^{-7}$  s, so that they decay far from the collision point, possibly outside the detector;
- c) their electric charge is either an integer or a fractional multiple of the proton charge.

Actually, quite a few theories beyond the SM foresee charged particles, both strongly and electroweakly interacting, with large masses and, although many exotic particles are unstable, often the lowest (or the next-to-lowest) lying state may be stable or quasi-stable [1, 2]. In the following, we call these states Massive Semi-stable Exotic Particles (MSEP's).

In the first part of this paper, we will briefly recall the difficulties which a large apparatus like ATLAS could meet while trying to detect MSEP's. In the second part, we show a concrete example of the measurements (involving detection, identification and track reconstruction) of MSEP's coming from supersymmetric models [3] with gauge-mediated supersymmetry breaking (GMSB) [4–6]. In this scheme, the supersymmetry (SUSY) [3] breaking occurs at relatively low energy scales, and it is mediated mainly by gauge interactions. The automatic suppression of the SUSY contributions to flavour-changing neutral currents and CP-violating processes is naturally fulfilled. Furthermore, in the simplest versions of GMSB, the Minimal Supersymmetric Standard Model (MSSM) spectrum and other observables depend on just five parameters, usually chosen to be [7–10]: the overall messenger scale  $M_{\text{mess}}$ , the so-called messenger index  $N_{\text{mess}}$ , the universal soft SUSY breaking scale felt by the low-energy sector  $\Lambda$ , the ratio of the vacuum expectation values of the two Higgs doublets  $\tan\beta$ , and  $\text{sign}(\mu)$ , which is the ambiguity left for the SUSY higgsino mass after imposing the conditions for a correct electroweak symmetry breaking.

In the following, we will consider GMSB models where the rôle of MSEP is taken by the stau (or all charged sleptons), which is the next-to-lightest SUSY particle (NLSP), decaying into gravitinos. These scenarios are very promising at the LHC, providing signatures of semi-stable charged tracks coming from massive sleptons, therefore with  $\beta$  often significantly smaller than 1. In particular, we perform our simulations at the ATLAS muon detector, whose excellent time resolution [11] allows a precision measurement of the slepton time of flight, and hence of the slepton velocity. We show that the event can be recognised with high efficiency by the calorimetric trigger requiring the usual SUSY signature of  $P_T^{\text{miss}} + \text{jets}$ , where the hadronic jets, originated by the decay of heavy squarks/gluinos along with MSEP's, must have the transverse momentum  $P_T > 50$  GeV and the transverse momentum imbalance  $P_T^{\text{miss}}$  is calculated only from the energy deposition in the hadronic calorimeter. It is remarkable that, in this framework, the event rate is very high and the background contamination due to SM channels can be reduced to a completely negligible level. Then, we conclude stressing the fact that the measurements of mass (using the MSEP momentum obtained by the muon system) and lifetime (obtained

by a counting method) are sufficient to determine the SUSY breaking scale  $\sqrt{F}$  at a level of precision of a few 10%'s.

Although this topic did not receive much attention up to now, as we will discuss, there is a sound theoretical basis to emphasise the physics and experimental search for MSEP's.

## 2 The Experimental Challenge

The experimental signatures of heavy long-lived charged particles at a hadron collider have been studied both in the framework of GMSB and in more general scenarios [12–15]. The two main observables one can use to separate these particles from muons are the high specific ionisation and the time of flight in the detector. As a matter of fact, a MSEP behaves like a massive muon with a velocity sometimes considerably lower than  $c$ . The energy loss of a MSEP in matter has been carefully studied in Ref. [16] (see also Ref. [1]), where it was shown that, for energy loss for ionisation when  $\beta > \frac{1}{2}$  and for particles with  $M > 100 \text{ GeV}/c^2$ , the range in iron exceeds several metres and increases with  $M$ . Moreover, for strongly interacting MSEP's the penetration length in matter does not change significantly for  $\beta \leq 0.7$  and  $M = 100 \text{ GeV}/c^2$  [16]. At the same time, a remarkable property of MSEP's is that, because of their low  $\beta$  value, they can produce anomalous energy loss for ionisation in matter that can be used as a distinctive feature for their identification.

Nevertheless, there are some drawbacks associated to low-velocity MSEP's. In fact, the detector synchronisation is tuned for particles travelling across the apparatus with the velocity of light, hence, due to the large geometrical dimensions of the typical LHC apparatus, all the data acquisition system should be carefully tuned in order to guarantee the trigger and the event reconstruction of a MSEP. The trigger system of the ATLAS experiment is described in detail in Ref. [11] (see Figs. 1 and 2 for schematic views of the ATLAS apparatus). Three levels of trigger are envisaged, which will reduce the initial input rate of 40 MHz for the first-level trigger progressively down to a rate of  $\sim 100$  Hz. This is the maximum input rate of the data storage system, and corresponds to an acquisition of  $\sim 100 \text{ MB/s}$ . The first level comes exclusively from the hardware, and the information from the muon detectors and from the calorimeters are treated separately. The second level refines the first level by connecting the information from different detectors. Finally, the third level (also called *event filter*) applies the full off-line reconstruction algorithms to the data.

The track identification of a MSEP escaping the hadronic calorimeter in the high  $p_T$  muon region is the natural task of the ATLAS specialised structure of muon precision chambers, composed by MDT's (Monitored Drift Tubes), which are dedicated to measure the trajectory of penetrating particles and to determine, with a good precision, the position of a charged particle.

We recall that in the central region an air-core toroidal superconducting magnet generates a magnetic field of about 0.5 T to allow the measurement of the particle momentum. The precision chambers are composed by two multilayers, and each of them is composed of three (four in the inner station) drift tube layers. A typical track goes through about twenty MDT's, before escaping from the apparatus. A single MDT is a cylindrical drift tube of 3 cm diameter. It is basically filled with Argon + CO<sub>2</sub> at 3 atmosphere absolute pressure. It has a typical spatial resolution  $\sigma = 80 \mu\text{m}$  and a maximum drift time of 700 ns. The resulting spatial resolution for the single particle is about  $30 \mu\text{m}$  [17]. Once an event has been accepted by the first level trigger, all the data coming from the MDT's for

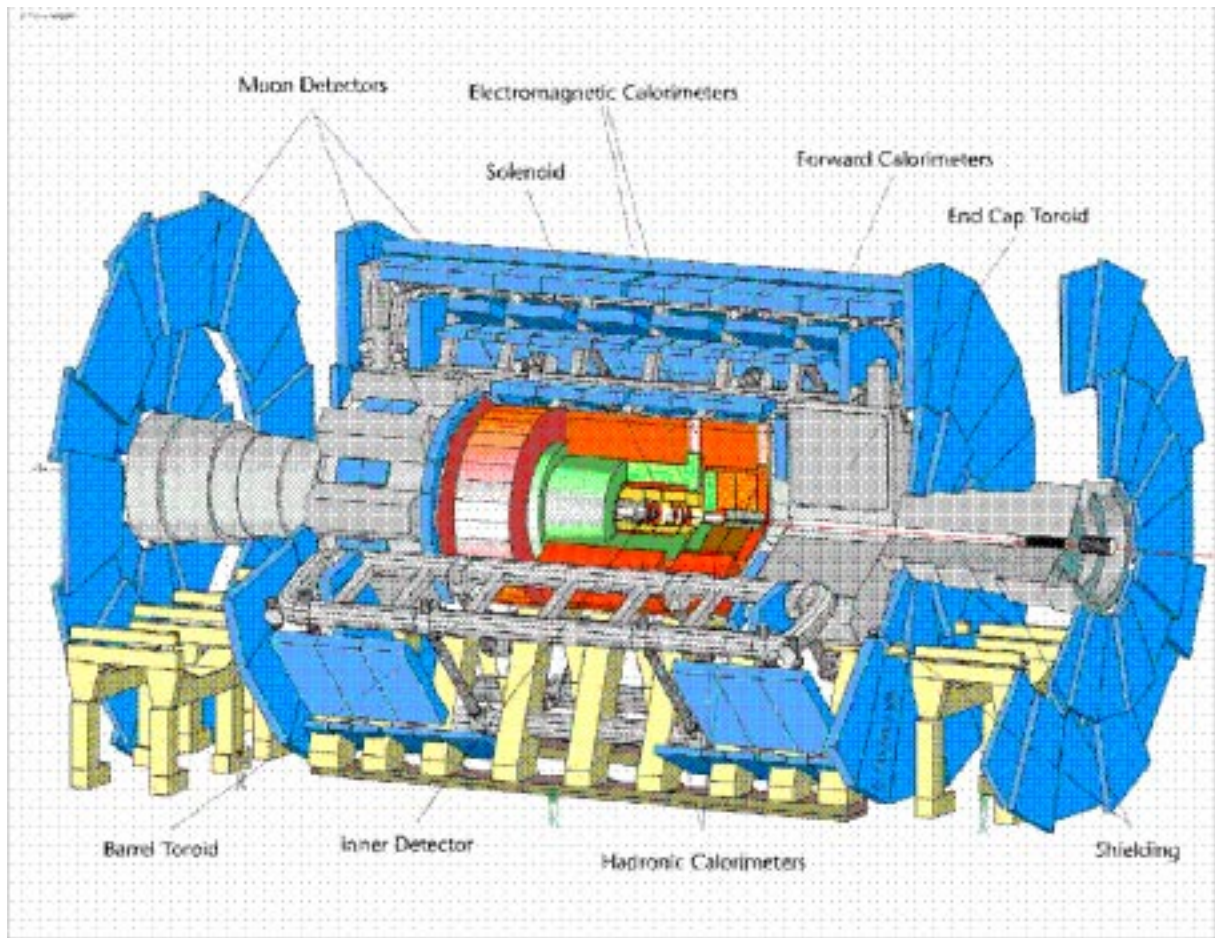


Figure 1: *Isometric view of the ATLAS detector with the description of the different functional parts.*

the following 700 ns are labelled with the same bunch crossing number and are extracted from the pipe-line memories. The track reconstruction for a MSEP will be done by taking into account in the hit analysis the delay along the track due to  $\beta < 1$ .

In our case, we will assume to trigger the MSEP's event by the hadronic calorimeter which can be easily activated by the multiple high  $P_T$  jets produced by the decay of squarks/gluinos with masses larger than 500 GeV together with MSEP's with masses of the order of 100 GeV. The classical SUSY signature of  $P_T^{\text{miss}} + \text{jets}$ , where  $P_T^{\text{miss}}$  is calculated only from the energy deposit in the calorimeter, neglecting the NLSP's and the muons, is in fact enough to pass the requests of the first level  $P_T^{\text{miss}}$  trigger of a jet with  $P_T > 50$  GeV and  $P_T^{\text{miss}} > 50$  GeV. A drawback of this purely calorimetric approach is the fact that processes with low hadronic activity, such as direct slepton production and direct electroweak gaugino production are not selected.

The measurements of the time of flight for MSEP's are made possible by the timing precision ( $\lesssim 1$  ns) and the size of the ATLAS muon spectrometer.

In the barrel part of the detector ( $|\eta| < 1$ ), the precision muon system consists of three multilayers of precision drift tubes immersed in a toroidal air-core magnetic field. The three measuring stations are located at distances of approximately 5, 7.5 and 10 m from the interaction point. A particle crossing a drift chamber ionises the chamber gas along its path, and the electrons produced by the ionisation drift to the anode wire under the influence of an electric field. The particle position is calculated from the measurement

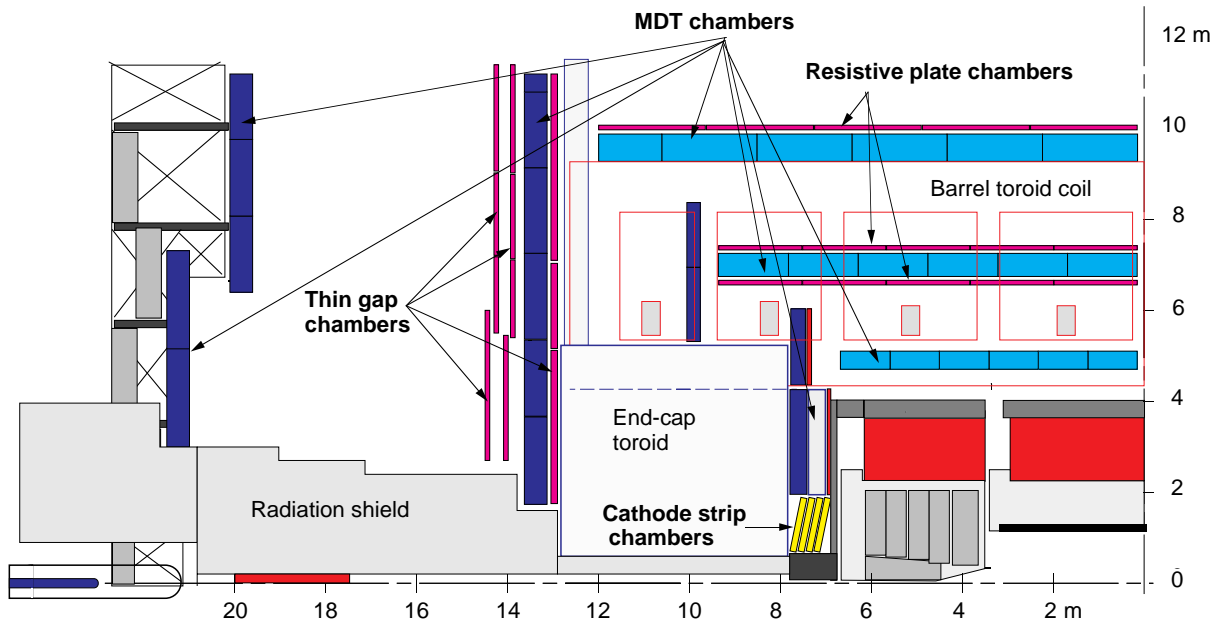


Figure 2: Side view of the ATLAS detector with the description of the different functional parts.

of the drift time of the ionisation electrons to the anode wire. In order to perform this calculation, a starting time  $t_0$  for counting the drift time is needed, corresponding to the time of flight of the particle from the production point to the measuring station. For a particle travelling approximately at the speed of light, as a muon, the  $t_0$ 's for the measuring stations are parameters of the detector geometry and of the response of the front-end electronics [18]. For a heavy particle, the  $t_0$  is a free parameter, function of the  $\beta$  ( $= v/c$ ) of the particle. It was demonstrated with a full simulation of the ATLAS muon detector [19] that the  $\beta$  of a particle can be measured by adjusting the  $t_0$  for each station in such a way to minimise the  $\chi^2$  of the reconstructed muon track.

The particle  $\beta$  can be measured with a resolution approximately parameterised as  $\sigma(\beta)/\beta^2 = 0.028$ . The resolution on the transverse momentum measurement for heavy particles is found to be comparable to the one expected for muons.

Besides the strong signature of the delay needed to reconstruct the track, a MSEP is identified by the energy loss for ionisation that can be much higher than that of a muon at minimum. This signature is a powerful physical quantity that gives a clear MSEP's identification.

As discussed in Ref. [12], already at  $\beta \sim 0.6$  the energy loss is around twice the minimum, and of course it increases rapidly for a lower value of  $\beta$ . A complete discussion of the ionisation measurement in the ATLAS detector is a very complicated problem which can not be addressed in this work. Here, we want to illustrate only in a preliminary way the possible rôle of the hadronic calorimeter and of the MDT's. We believe that the calorimeter can bring a significant contribution to the identification of MSEP's. The ATLAS hadron calorimeter can measure the muon energy deposit with an accuracy of about 25%, in the last compartment, and  $\sim 20\%$ , using the full depth. The contamination induced by the minimum bias event pile-up is expected to be of the order of 1% or lower at full luminosity.

In the case of the MDT detector, the measurement of total charge based on a single MDT appears poor because of the background contamination at full LHC luminosity.

Notwithstanding, measurement of charge performed by a statistical procedure involving the complete set of  $\sim 20$  tubes fired by the particle can provide a significantly improved measurement. It must be considered that the MDT's front-end electronics is optimised to provide a charge integration only for a small fraction of the total drift time ( $\sim 30$  ns). However, even with this limitation, it could be possible that again the statistical combination of all the tubes belonging to the track can provide a good ionisation measurement.

Of course, this brief discussion does not exhaust all the possibilities offered by the ATLAS apparatus. For example, it was shown in Ref. [11] that the ionisation energy loss measurement in the Transition Radiation Tracker can be used to achieve  $\pi/K$  separation and, in some cases, the electromagnetic calorimeter can provide the charge measurements.

### 3 Supersymmetric Scenario

The phenomenology of GMSB (and more in general of any theory with low-energy SUSY breaking) is characterised by the presence of a very light gravitino  $\tilde{G}$  [20],

$$m_{3/2} \equiv m_{\tilde{G}} = \frac{F}{\sqrt{3}M'_P}, \quad (1)$$

where  $\sqrt{F}$  is the fundamental scale of SUSY breaking. If we assume the typical value  $\sqrt{F} = 100$  TeV, and  $M'_P = 2.44 \times 10^{18}$  GeV for the reduced Planck mass, we get  $m_{3/2} = 2.37$  eV. Hence,  $\tilde{G}$  is always the lightest SUSY particle (LSP) in these theories. If  $R$ -parity is assumed to be conserved, any produced MSSM particle will finally decay into the gravitino. Depending on  $\sqrt{F}$ , the interactions of the gravitino, although much weaker than gauge and Yukawa interactions, can still be strong enough to be of relevance for collider physics. As a result, in most cases the last step of any SUSY decay chain is the decay of the next-to-lightest SUSY particle (NLSP), which can occur outside or inside a typical detector (even close to the interaction point). The pattern of the resulting spectacular signatures is determined by the identity of the NLSP and its lifetime before decaying into  $\tilde{G}$ ,

$$\frac{c\tau_{\text{NLSP}}}{\text{cm}} \simeq \frac{1}{100\mathcal{B}} \left( \frac{\sqrt{F}}{100 \text{ TeV}} \right)^4 \left( \frac{m_{\text{NLSP}}}{100 \text{ GeV}} \right)^{-5}, \quad (2)$$

where  $\mathcal{B}$  is a number of order unity depending on the nature of the NLSP. The identity of the NLSP [or, to be more precise, the identity of the sparticle(s) having a large branching ratio (BR) for decaying into the gravitino and the relevant SM partner] determines four main scenarios giving rise to qualitatively different phenomenology: a) the Neutralino-NLSP Scenario; b) the Stau-NLSP Scenario; c) the Slepton co-NLSP Scenario; d) the Neutralino-Stau co-NLSP Scenario [9]. In this paper, we will be concerned with Scenarios b) and c) only.

The two main parameters affecting the experimental measurement at the LHC of the slepton NLSP properties are the slepton mass and momentum distribution. Indeed, at a hadron collider most of the NLSP's come from squark and gluino production, followed by cascade decays. Thus, the momentum distribution is in general a function of the whole MSSM spectrum. However, one can approximately assume that most of the information on the NLSP momentum distribution is provided by the squark mass scale  $m_{\tilde{q}}$  only (in the stau NLSP scenario or slepton co-NLSP scenarios of GMSB, one generally finds  $m_{\tilde{g}} \gtrsim m_{\tilde{q}}$ ). To perform detailed simulations, we select a representative set of GMSB models generated

Model	1	2	3	4	5	6	7	8
$M_{\text{mess}} (10^4 \text{ TeV})$	1.79	5.28	0.0436	0.0151	3.88	23.1	75.7	0.0479
$N_{\text{mess}}$	3	3	5	4	6	3	3	5
$\Lambda (\text{TeV})$	26.6	26.0	41.9	28.3	58.6	65.2	104	71.9
$\tan \beta$	7.22	2.28	53.7	1.27	41.9	1.83	8.54	3.27
$\text{sign}(\mu)$	-	-	+	-	+	-	-	-
$m_{\tilde{\tau}_1=\text{NLSP}} (\text{GeV})$	100.1	100.4	101.0	103.4	251.2	245.3	399.2	302.9
“NLSP” Scenario	$\tilde{\tau}_1$	$\tilde{\ell}$	$\tilde{\tau}_1$	$\tilde{\ell}$	$\tilde{\tau}_1$	$\tilde{\ell}$	$\tilde{\tau}_1$	$\tilde{\ell}$
$m_{\tilde{q}} (\text{GeV})$	577	563	1190	721	1910	1290	2000	1960
$m_{\tilde{g}} (\text{GeV})$	631	617	1480	859	2370	1410	2170	2430
$\sigma (\text{pb})$	42	50	0.59	10	0.023	0.36	0.017	0.022
SUSY events	452163	528420	7437	147354	365	6535	326	378
BKGD: $W$ +Jets	9.6	9.6	9.5	9.5	2.4	2.4	1.0	1.8
BKGD: $Z$ +Jets	6.8	6.9	6.9	7.1	11.1	11.0	5.9	8.7
BKGD: $t\bar{t}$	5.3	5.3	5.3	5.6	6.2	6.5	3.4	4.9
BKGD: QCD	8.0	8.0	8.0	7.4	3.1	3.1	0.5	2.0
BKGD: Total	29.7	29.9	29.9	29.9	22.8	23.0	10.8	17.4

Table 1: In rows 1–5, the input parameters of the eight sample GMSB models chosen for our study are reported. In rows 6–10, the main features of the models ( $\tilde{\ell} = \tilde{e}_R, \tilde{\mu}_R, \tilde{\tau}_1$ ) are shown. The average squark mass is indicated by  $m_{\tilde{q}}$  and  $m_{\tilde{g}}$  is the gluino mass. In the last six rows, the comparison among the expected number of events after the cuts described in Sect. 3.1 and the major background sources are reported. The assumed integrated luminosity is  $30 \text{ fb}^{-1}$ , corresponding to a three-year low-luminosity run at the LHC. In the table, BKGD is a shorthand for “background”, and  $M_{\text{mess}}$  and  $N_{\text{mess}}$  are defined in the text (see Refs. [6–10]).

by SUSYFIRE [21]. We limit ourselves to models with  $m_{\text{NLSP}} > 100 \text{ GeV}$ , that cannot be excluded by direct searches at LEP/Tevatron, and  $m_{\tilde{q}} < 2 \text{ TeV}$ , in order to yield an adequate event statistics after a three-year low-luminosity run (corresponding to  $30 \text{ fb}^{-1}$ ) at the LHC. Within these ranges, we choose eight extreme points (four in the stau NLSP scenario and four in the slepton co-NLSP scenario) allowed by GMSB in the  $(m_{\text{NLSP}}, m_{\tilde{q}})$  plane, in order to cover the various possibilities. More details can be found in Refs. [22, 23]. In Tab. 1 (first five rows), we list the input GMSB parameters we used to generate these eight points.

### 3.1 Event Selection and Slepton Mass Measurement

In order to select a clean sample of sleptons, we applied the following requirements:

- at least a hadronic jet with  $P_T > 50 \text{ GeV}$  and a calorimetric  $E_T^{\text{miss}} > 50 \text{ GeV}$  (trigger requirement);
- at least one slepton candidate satisfying the following cuts:
  - $|\eta| < 2.4$  to ensure that the particle is in the acceptance of the muon trigger chamber, and therefore both coordinates can be measured;



- $\beta_{\text{meas}} < 0.91$ , where  $\beta_{\text{meas}}$  is the  $\beta$  of the particle measured with the time of flight in the precision chambers;
  - The  $P_T$  of the slepton candidate, after the energy loss in the calorimeters has been taken into account, must be larger than 10 GeV, to ensure that the particle traverses all the muon stations.
- a cut  $m_{\text{eff}} > 800$  GeV, where  $m_{\text{eff}}$  is the total invariant mass of the event constructed starting from the transverse momentum of the high  $P_T$  jets and muons (or muon-like particles) [23].

Considering an integrated luminosity of  $30 \text{ fb}^{-1}$ , a number of events ranging from a few hundred, for the models with 2 TeV squark-mass scale, to a few hundred thousand, for a 500 GeV mass scale, survives these cuts. These events can be used to measure the NLSP properties. For the sake of comparison, we recall that about 1500 events for a light Higgs boson production are expected in the channel  $H \rightarrow \gamma\gamma$  in the same environment [11].

In order to perform the mass measurement, the particle momentum is needed. The precision chambers only provide a measurement of the momentum components transverse to the beam axis, so a measurement of the slepton pseudorapidity is necessary. This can be performed either by a match with a track in the inner detector, or using the information from the muon trigger chambers. The first option requires a detailed study of the matching procedure between detectors. This study was performed for muons in Ref. [11], but the results can not be transferred automatically to the case of heavy particles for which the effect of multiple scattering in crossing the calorimetric system is much more severe.

In the case of the trigger chambers, a limited time window around the beam crossing is read out, restricting the  $\beta$  range for which the momentum can be measured. We therefore evaluated the statistical precision achievable for the eight example models in two different  $\beta$  intervals:  $0.6 < \beta < 0.91$  and  $0.8 < \beta < 0.91$ .

Many more technical details about this analysis can be found in Refs. [22, 23].

### 3.2 Slepton Lifetime Measurement and $\sqrt{F}$

The measurement of the slepton NLSP lifetime was performed by exploiting the fact that a couple of NLSP's is produced in each event. We adopted a method similar to the one used in Ref. [10] for the high energy  $e^+e^-$  collider in the neutralino NLSP case.

This method consists in selecting the  $N_1$  events where a slepton is detected through the time-of-flight measurement and then counting how many times ( $N_2$ ) a second slepton is observed. This information is sufficient to determine the lifetime. Although in principle very simple, in practice this method requires an excellent control of all possible sources of inefficiency for detecting the second slepton.

The first set of  $N_1$  events is defined with the additional requirement that, for a given value of the slepton lifetime, at least one of the produced sleptons decays at a distance from the interaction vertex  $> 10$  m, and is therefore reconstructed in the muon system. For the events thus selected, we define  $N_2$  as the number of events in the subsample where a second particle with transverse momentum  $> 10$  GeV is identified in the muon system. The search for the second particle should be as inclusive as possible, in order to minimise the corrections to the ratio

$$R = \frac{N_2}{N_1}, \quad (3)$$

which is a function of the slepton lifetime. Its dependence on the NLSP lifetime  $c\tau$  in meters is shown in Fig. 3 for four out of the eight sample models.

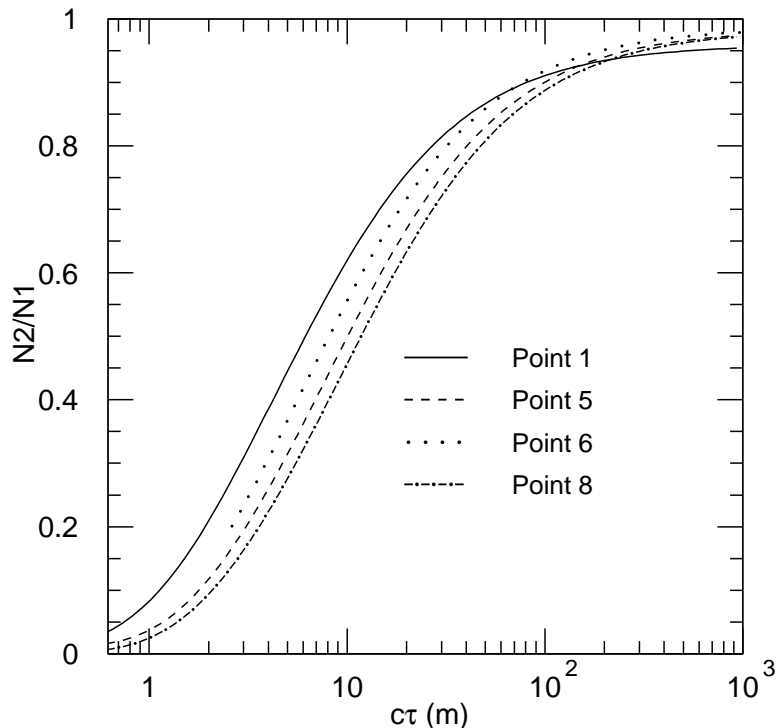


Figure 3: The ratio  $R = N_2/N_1$  defined in the text as a function of the slepton lifetime  $c\tau$ . The curves corresponding to the model points 1, 5, 6, 8 are shown.

The probability for a particle of mass  $m$ , momentum  $p$  and proper lifetime  $\tau$  to travel for a distance  $L$  before decaying is given by  $P(L) = e^{-mL/pc\tau}$ .  $N_2$  is therefore a function of the momentum distribution of the slepton, which is determined by the details of the SUSY spectrum. One needs therefore to be able to simulate the full SUSY cascade decays in order to construct the  $c\tau$ – $R$  relationship.

Relevant for the precision of the SUSY breaking scale measurement is the error on the measured  $c\tau$ . This can be extracted from the curves shown in Fig. 3.

The precision calculated according to this formula is shown in Fig. 4 (left side), for model sample point 1 and an integrated luminosity of  $30 \text{ fb}^{-1}$ . The full line in the plot is the error on  $c\tau$  considering the statistical error on  $R$  only. The available statistics is a function of the strongly interacting sparticle mass scale.

We parameterise the systematic error as a term proportional to  $R$ , added in quadrature to the statistical error. We choose two values,  $1\%R$  and  $5\%R$ , and propagate the error to the  $c\tau$  measurement. The results are represented by the dashed and dotted lines in Fig. 4 (left side).

For the models with squark mass scales up to 1200 GeV, assuming a 1% systematic error on the measured ratio, a precision better than 10% on the  $c\tau$  measurement can be obtained for lifetimes between 0.5–1 m and 50–80 m. If the systematic uncertainty grows up to 5%, the 10% precision can only be achieved in the range 1–10 m. If the mass scale goes up to 2 TeV, even considering a pure statistical error only, a 10% precision is not achievable. However a 20% precision is possible over  $c\tau$  ranges between 5 and 100 m, assuming a 1% systematic error.

Using the measured values of  $c\tau$  and the NLSP mass, the SUSY breaking scale  $\sqrt{F}$  can

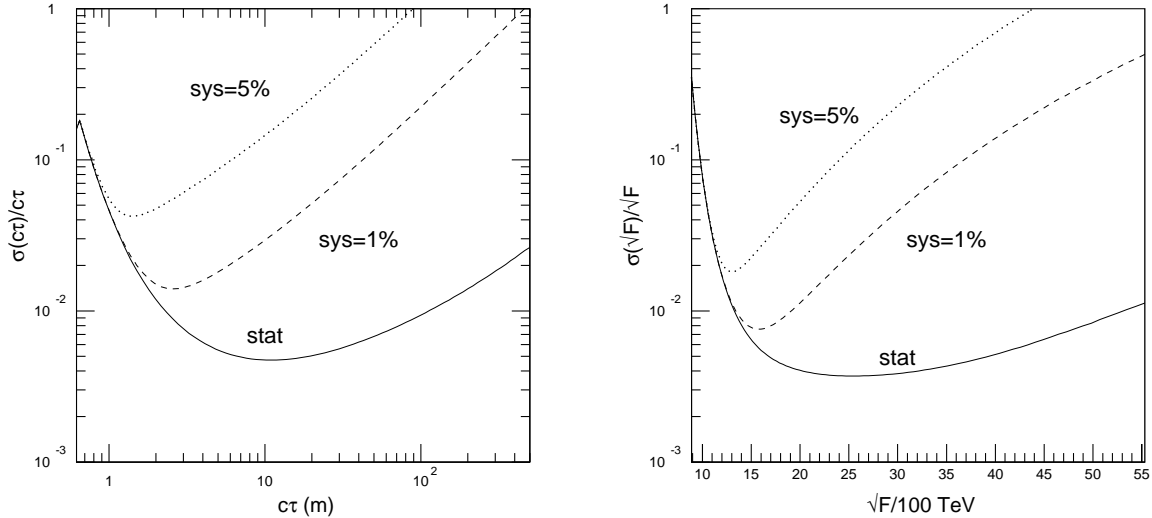


Figure 4: *Fractional error on the measurements of the slepton lifetime  $c\tau$  (left side) and the SUSY breaking scale (right side), for model sample point 1 only. We assume an integrated luminosity of  $30 \text{ fb}^{-1}$ . The curves are shown for three different assumptions on the fractional systematic error on the  $R$  measurement: statistical error only (full line), 1% systematic error (dashed line), 5% systematic error (dotted line).*

be calculated from Eq. (2), where  $\mathcal{B} = 1$  for our case where the NLSP is a slepton. The fractional uncertainty on the  $\sqrt{F}$  measurement can be obtained adding in quadrature one fourth of the fractional error in  $c\tau$  and five fourths of the fractional error on the slepton mass. In Fig. 4 (right side), we show the fractional error on the  $\sqrt{F}$  measurement as a function of  $\sqrt{F}$  for our three different assumptions on the  $c\tau$  error. The uncertainty is dominated by  $c\tau$  for the upper part of the  $\sqrt{F}$  range, and grows quickly when approaching the lower limit on  $\sqrt{F}$ . This is because very few sleptons survive and the statistical error on both  $m_{\tilde{\ell}}$  and  $c\tau$  gets very large. The error on  $\sqrt{F}$  is better than 10% for  $1000 \lesssim \sqrt{F} \lesssim 4000 \text{ TeV}$ .

## 4 Conclusions

We have shown how the ATLAS detector at the LHC can be used to detect and measure the mass and lifetime of massive long-lived charged particles produced in the framework of supersymmetric models with gauge-mediated SUSY breaking, where a slepton is the NLSP and decays into a gravitino with a lifetime in the range  $0.5 \text{ m} \lesssim c\tau_{\text{NLSP}} \lesssim 1 \text{ km}$ . At the LHC, a large amount of SUSY particles of this kind is generated, while the SM background can be reduced at a very low level with appropriate cuts.

The lifetime measurement can be performed by a counting method with a good accuracy, allowing the computation of the value of the SUSY breaking scale  $\sqrt{F}$ .

The peculiar problems of the MSEP detection, related with the event trigger and the time-of-flight measurement, have been discussed. The delicate point of the possibility of measuring the specific ionisation by the MDT's and by different sectors of the hadronic calorimeter has been addressed. We stressed the importance that the specific ionisation measurements have for a clear MSEP identification.

# References

- [1] S. Errede and S. H. H. Tye, in Proc. of the 1984 Summer Study on the Design and Utilization of SSC, Snowmass, Colorado, 1984, J. Morfin and R. Donaldson eds., pag. 175.
- [2] K. Enqvist, K. Mursula, M. Roos, Nucl. Phys. **B226** (1983) 121.
- [3] S. P. Martin, “A Supersymmetry Primer”, in “Perspectives on Supersymmetry”, G. L. Kane ed., World Scientific 1998, hep-ph/9709356, and references therein.
- [4] M. Dine, W. Fischler, M. Srednicki, Nucl. Phys. **B189** (1981) 575; S. Dimopoulos, S. Raby, Nucl. Phys. **B192** (1981) 353; M. Dine, W. Fischler, Phys. Lett. **110B** (1982) 227; M. Dine, M. Srednicki, Nucl. Phys. **B202** (1982) 238; M. Dine, W. Fischler, Nucl. Phys. **B204** (1982) 346; L. Alvarez-Gaumé, M. Claudson, M. B. Wise, Nucl. Phys. **B207** (1982) 96; C. R. Nappi, B. A. Ovrut, Phys. Lett. **113B** (1982) 175; S. Dimopoulos, S. Raby, Nucl. Phys. **B219** (1983) 479.
- [5] M. Dine, A. E. Nelson, Phys. Rev. D **48** (1993) 1277; M. Dine, A. E. Nelson, Y. Shirman, Phys. Rev. D **51** (1995) 1362; M. Dine, A. E. Nelson, Y. Nir, Y. Shirman, Phys. Rev. D **53** (1996) 2658.
- [6] G. F. Giudice, R. Rattazzi, “Theories with Gauge-Mediated Supersymmetry Breaking”, Phys. Rep. **322** (1999) 419-499, 501.
- [7] S. Dimopoulos, S. Thomas, J. D. Wells, Phys. Rev. D **54** (1996) 3283; Nucl. Phys. **B488** (1997) 39.
- [8] J. A. Bagger, K. Matchev, D. M. Pierce, R. Zhang, Phys. Rev. D **55** (1997) 3188.
- [9] S. Ambrosanio, G. D. Kribs, S. P. Martin, Phys. Rev. D **56** (1997) 1761.
- [10] S. Ambrosanio, G. A. Blair, Eur. Phys. J. C **12** (2000) 287–321.
- [11] The ATLAS Collaboration, “ATLAS Detector and Physics Performance Technical Design Report”, ATLAS TDR 15, CERN/LHCC/99-15, CERN Library, Geneva, Switzerland, 1999.
- [12] A. Nisati, S. Petrarca, G. Salvini, Mod. Phys. Lett. **A12** (1997) 2213; S. Petrarca and G. Salvini, “Search for Stable Exotic Massive Particles at LHC by an Instrumented Air-Core Toroid (ASCOT type)”, Dip. di Fisica, Università di Roma “La Sapienza”, Nota Interna n. 999 (1992).
- [13] M. Drees, X. Tata, Phys. Lett. B **252** (1990) 695.
- [14] J. L. Feng, T. Moroi, Phys. Rev. D **58** (1998) 035001.
- [15] S. P. Martin, J. D. Wells, Phys. Rev. D **59** (1999) 035008.
- [16] M. Drees and X. Tata, Phys. Lett. B **252** (1990) 695.
- [17] The ATLAS Collaboration, “Muon Spectrometer Technical Design Report”, CERN/LHCC/97-22, CERN Library, Geneva, Switzerland, 1997.

- [18] A. Nisati, “Preliminary Timing Studies of the Barrel Muon Trigger System”, ATLAS Internal Note ATL-DAQ-98-083, CERN Library, Geneva, Switzerland, 1998.
- [19] G. Polesello, A. Rimoldi, “Reconstruction of Quasi-stable Charged Sleptons in the ATLAS Muon Spectrometer”, ATLAS Internal Note ATL-MUON-99-06, CERN Library, Geneva, Switzerland, 1999.
- [20] P. Fayet, Phys. Lett. **70B** (1977) 461; Phys. Lett. **86B** (1979) 272; Phys. Lett. B **175** (1986) 471 and in “Unification of the fundamental particle interactions”, S. Ferrara, J. Ellis, P. van Nieuwenhuizen eds. (Plenum, New York, 1980), p. 587.
- [21] An updated, generalised and **Fortran**-linked version of the program used in Ref. [9]. It generates minimal and non-minimal GMSB and SUGRA models. For inquiries about this software package, please send e-mail to `ambros@mail.cern.ch`.
- [22] S. Ambrosanio, B. Mele, S. Petrarca, G. Polesello, A. Rimoldi, in “Aspects of GMSB Phenomenology at TeV Colliders”, in hep/ph-0002191 and hep/ph-0005142, Summary Report of the SUSY Working Group, Workshop on Physics at TeV Colliders, Les Houches, France, 7-18 June 1999.
- [23] S. Ambrosanio, B. Mele, S. Petrarca, G. Polesello, A. Rimoldi, “Measuring the SUSY Breaking Scale at the LHC in the Slepton NLSP Scenario of GMSB Models”, hep-ph/0010081, submitted to *The Journal of High-Energy Physics*.